Physical Communication 25 (2017) 519–526

Contents lists available at ScienceDirect

Physical Communication

journal homepage: www.elsevier.com/locate/phycom

Full length article

A comprehensive framework for Double Spatial Modulation under imperfect channel state information

Goutham Simha G.D. [a,*], Shriharsha K. [b], Raghavendra M.A.N.S. [a], U. Shripathi Acharya [a]

[a] Electronics and Communications, National Institute of Technology Karnataka, Surathkal, India
[b] Smart IOPS solutions Pvt Ltd., Bengaluru, India

ARTICLE INFO

Article history:
Received 30 April 2017
Received in revised form 29 July 2017
Accepted 16 October 2017
Available online 2 November 2017

Keywords:
Index modulation (IM)
Spatial modulation (SM)
Double spatial modulation (DSM)
Average bit error probability (ABEP)
Perfect channel state information (P-CSI)
Imperfect channel state information (Imp-CSI)

ABSTRACT

The essential requirement for a 5G wireless communication system is the realization of energy efficient as well as spectrally efficient modulation schemes. Double Spatial Modulation (DSM) is a recently proposed high rate Index Modulation (IM) scheme, designed for use in Multiple Input Multiple Output (MIMO) wireless systems. The aim of this scheme is to increase the spectral efficiency of conventional Spatial Modulation (SM) systems while keeping the energy efficiency intact. In this paper, the impact of imperfect channel knowledge on the performance of DSM system under Rayleigh, Rician and Nakagami-m fading channels has been quantified. Later, a modified low complexity decoder for the DSM scheme has been designed using ordered block minimum mean square error (OB-MMSE) criterion. Its performance under varied fading environments have been quantified via Monte Carlo simulations. Finally, a closed form expression for the pairwise error probability (PEP) for a DSM scheme under conditions of perfect and imperfect channel state information has been derived. This is employed to calculate the upper bound on the average bit error probability (ABEP) over aforementioned fading channels. It is observed that, under perfect and imperfect channel conditions DSM outperforms all the other variants of SM by at least 2dB at an average bit error ratio (ABER) of 10^{-5}. Tightness of the derived upper bound is illustrated by Monte Carlo simulation results.

1. Introduction

In the era of modern wireless communications, the MIMO innovation has enabled the development of a large number of services (live video streaming, e-commerce applications, LTE to vehicular communications etc.). These applications require the underlying network to be highly spectrally efficient and the mobile platforms to be computationally capable and energy efficient. The MIMO paradigm has brought significant improvements in reliability and throughput of wireless systems when compared to the earlier Single Input Single Output (SISO) framework. To fulfill the ever increasing demand for higher information throughput, innovations in MIMO such as Spatial Multiplexing (SMX) and its various derivatives have been proposed. Space Time Codes (STC) have been synthesized with the goal of achieving improved reliability at a given throughput [1–3]. Considering the exigent objectives for next generation 5G wireless communication systems, researchers have propounded intelligent and novel physical layer modulation techniques. One of the examples is a high rate spectrally efficient Index Modulation (IM) scheme used in large MIMO, massive MIMO and non-orthogonal multi-carrier systems [4]. An important breakthrough in the design of Space Time (ST) techniques was the discovery of Spatial Modulation (SM) by Mesleh et al. [5], which demonstrated that spectral efficiency along with energy efficiency could be simultaneously achieved by selecting only one antenna at a time out of the available antennas and assigning bits to the selecting antenna, the notion of antenna selection bits and information bits was introduced. This technique allowed the designer to reduce the number of RF chains, thus improving the energy efficiency. Spectral efficiency was enhanced by communicating some information through the medium of antenna selection bits which are not physically communicated [5,6]. This scheme is amalgamated as a part of MIMO wireless communication system to expand the spectral efficiency and reliability. It also nullifies Inter Channel Interference (ICI) due to its inherent way of choosing only one antenna at a time during the process of transmission. Furthermore, ICI and inter antenna synchronization can be eliminated completely by activating a single RF chain at a time [7,8] . To extend the spectral efficiency in SM-MIMO systems Younis et al., came up with the idea of Generalized Spatial Modulation (GNSM) in which the number of active antennas is increased to two [9]. The primary

* Corresponding author.
E-mail addresses: ec12f04.goutham@nitk.edu.in (Goutham Simha G.D.), bhatshri29@gmail.com (Shriharsha K.), rma.11ce24f@nitk.edu.in (Raghavendra M.A.N.S.), shripathi.acharya@nitk.edu.in (U.S. Acharya).

https://doi.org/10.1016/j.phycom.2017.10.010
1874-4907/

limitation of this scheme when compared with conventional SM is its requirement of more than one RF chain [9]. SM systems enable a logarithmic improvement in the multiplexing gain with an increase in the number of antennas. A new technique was proposed by Mesleh et al. [10] known as the Quadrature Spatial Modulation (QSM) which retains the structural features of conventional SM systems, while providing an improvement in spectral efficiency. In order to improve the performance over conventional SM systems, a Euclidean distance based Enhanced Spatial Modulation (ESM) was developed by Cheng et al. [11]. In this technique active antenna combinations vary as one or two. The ESM technique uses primary constellation points if one antenna is active and employs secondary constellation if two antennas become active. In order to associate identical number of antenna bits with every antenna combination, the spacing between the constellation points of the secondary constellation is chosen to be half the number of points of the primary constellation. (16QAM,4QAM), (4QAM,BPSK) are some specific examples of primary and secondary constellations [11]. It has been shown with proper analytical reasoning that QSM systems outperform SM systems in almost all uncorrelated fading environments under conditions of identical spectral efficiency and antenna number [12]. Younis et al. proposed a performance study of QSM systems over Nakagami-*m* fading channels which enumerates the advantages of QSM systems over SM systems in different non uniform Nakagami-*m* fading channels [13]. In order to have a twofold increase in spectral efficiency as compared to traditional SM scheme, Zehra and Basar proposed a high rate IM scheme for use in MIMO and large MIMO systems which is designated as Double Spatial Modulation (DSM) [14]. The primary advantage of this technique is that it allows the activation of more than one antenna which leads to higher spectral efficiency. This scheme can allow an improvement in spectral efficiency from 10 bps/Hz to 16 bps/Hz which is a requirement in 5G wireless communication environment. In DSM scheme, the first bit splitter splits the incoming data bits into two SM streams. The upper SM configuration processes bits provided to it in the conventional manner. Bits fed to the lower block are processed by an SM configuration which employs an optimally rotated signal constellation of identical size. This has been done exclusively to improve the ease of detection [14]. ML decoding is optimum but has the disadvantage of requiring a large number of computations. Yue Xiao et al. proposed a low complexity decoding technique known as the ordered block minimum mean squared error (OB-MMSE), which achieves near ML execution with eighty percent reduction in computational complexity [15].

The primary focus and the contributions of this paper are broadly classified as follows:

- To propose a framework for the contemporary high rate index modulated DSM scheme under conditions of perfect and imperfect channel information over Rayleigh, Rician and Nakagami-*m* fading channels.
- For any MIMO system, a more adaptable and pragmatic framework can be obtained by implementing non uniform phase distribution of Nakagami-*m* channel as given in [16]. A special case study of the DSM scheme under Nakagami-*m* fading environment with Perfect (P-CSI) and Imperfect (Imp-CSI) is described and simulated. This is to quantify the performance of DSM scheme in Nakagami-*m* fading environment under conditions of non uniform phase distribution for different *m*.
- To design and evaluate the performance of a modified low complexity OB-MMSE signal detector for a DSM system over ML detection.

The rest of this paper is organized as follows: In Section 2, we describe the system and channel models. An analytical treatment (closed form expression for ABER under Rician and Nakagami-*m* fading in addition to Rayleigh) for DSM scheme is given in Section 3. This is followed by Monte Carlo simulation results and performance comparisons in Section 4. The paper is finally concluded in Section 5.

2. System and channel model

The system model of a DSM (high rate index modulated) scheme is shown in Fig. 1 [14]. The system under consideration is in the form of $N_t \times N_r$ MIMO arrangement where N_t denotes the number of transmit antennas, N_r is the number of receive antennas and M is the constellation order. The spectral efficiency of this scheme is defined to be $\log_2(N_t^2 M^2)$ bpcu. Let us consider that $\log_2(N_t^2 M^2)$ are to be transmitted. Bit splitter-1 arrangement divides these bits into two equal halves. Each stream contains $\log_2(N_t M)$ bits. From this arrangement, it is apparent that DSM can be viewed as two individual SM systems working in tandem. Later, bit splitter-2 splits the data symbols into information bearing bits and antenna indexing bits. At this stage, the $\log_2(M)$ bits constitute to information bits and $\log_2(N_t)$ bits represent antenna selection bits respectively. It can be inferred from Figure.1 that, the first information symbol s_1 is directly radiated from the transmit antenna indexed as A_1. The second information symbol s_2 is rotated by an optimum angle θ (which depends upon the constellation) prior to transmission over the second active transmit antenna indexed as A_2. To minimize bit error rate, the optimized rotation angle θ has been determined for commonly used MQAM constellations [14]. The transmission vector $\mathbf{S} \epsilon \mathbb{C}^{\mathbf{N_t}\times\mathbf{1}}$ is of the form

$$\mathbf{S} = [0 \cdots \underbrace{\mathbf{s_1}}_{A_1} \cdots 0 \cdots \underbrace{\mathbf{s_2} e^{j\theta}}_{A_2} \cdots 0 \cdots 0]^T \tag{1}$$

vector $\mathbf{S}$ is transmitted over a frequency flat MIMO channel of size N_t. Let $\mathbf{H}$ be a $N_r \times N_t$ channel matrix, $\mathbf{n}$ is a column vector containing circularly symmetric complex Gaussian number as elements $C\,\mathcal{N}(0, \sigma^2)$. The elements of $\mathbf{n}$ are assumed to be independent and identically distributed (i.i.d).

The received signal can be characterized by

$$\mathbf{Y} = \mathbf{H}\,\mathbf{S} + \mathbf{n};\ \ \boldsymbol{Y} = \mathbf{h_{A_1}} \mathbf{s_1} + \mathbf{h_{A_2}} \mathbf{s_2} \mathbf{e^{j\theta}} + \mathbf{n} \tag{2}$$

where $\mathbf{Y}$ is a $\mathbb{C}^{N_r \times 1}$ matrix, $\mathbf{n} \epsilon \mathbb{C}^{\mathbf{N_r}\times\mathbf{1}}$ is AWGN, $\mathbf{h_{A_1}}$ and $\mathbf{h_{A_2}}$ indicate the column vectors of $\mathbf{H}$ corresponding to active antenna indices (A_1, A_2).

The performance analysis of spectrally efficient DSM scheme over Rayleigh, Rician and Nakagami-*m* fading channels with P-CSI and Imp-CSI is analytically derived and quantified. Later, as a special case we have studied the characteristics of DSM scheme under Nakagami-*m* fading environment for uniform and non uniform distribution. The following subsections describe the channel models for various fading environments.

2.1. Rayleigh and Rician fading channels

The channel matrix is constructed as given in [17,18]. Realization of both Rayleigh and Rician fading channels in uncorrelated and correlated scenarios is presented.

$$\mathbf{H} = \check{\mathbf{H}} + \dot{\mathbf{H}} \tag{3}$$

where $\check{\mathbf{H}}$ is the mean matrix and $\dot{\mathbf{H}}$ is a $N_r \times N_t$ matrix which is $C\,\mathcal{N}(0, 1)$. $\dot{\mathbf{H}}$ matrix may be uncorrelated or correlated depending upon the fading scenario and antenna separation in an array. Under correlated channel conditions auxiliary terms from the Kronecker model gets multiplied to $\mathbf{H}$ and final equation reduces to (4) as given in [9,17].

$$\dot{\mathbf{H}} = \mathbf{H_c} = \mathbf{R_{REC}^{1/2}} \cdot \mathbf{H} \cdot \mathbf{R_{TRAN}^{1/2}}. \tag{4}$$

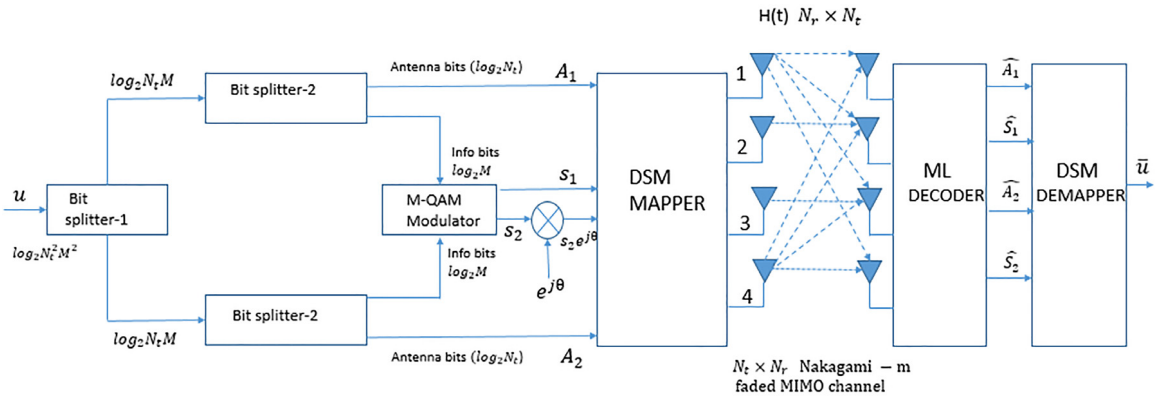

Fig. 1. Block diagram for DSM system [14].

In this equation, $\mathbf{H_c}$ denotes a correlated channel matrix, $\mathbf{H}$ indicates a channel matrix with Rayleigh fading having dimension $N_r \times N_t$. $\mathbf{R_{TRAN}}$ has information about the correlation between different antenna elements of the transmit array. This is termed as the transmit correlation matrix. $\mathbf{R_{REC}}$ specifies the correlation between various elements of the receive antenna array. This is referred to as the receive correlation matrix. The mean matrix for a Rayleigh fading channel can be calculated from [9] as $\check{\mathbf{H}} = \mathbf{0}_{N_r \times N_t}$ matrix.

The entries of the Rician channel matrix $\mathbf{H}$ are modeled as given in [9,17] as,

$$\mathbf{H} = \sqrt{\frac{K}{1+K}}\check{\mathbf{H}} + \sqrt{\frac{1}{1+K}}\bar{\mathbf{H}}. \tag{5}$$

For a Rician fading channel the mean matrix is expressed as

$$\check{\mathbf{H}} = \sqrt{\frac{K}{1+K}} \times \mathbf{1}_{N_r \times N_t} \tag{6}$$

where K denotes the Rician factor, $K/(1+K)$ constitutes to average power of the LOS component, $\check{\mathbf{H}}$ is the mean matrix and is defined as matrix of all ones, $1/(1+K)$ is the average power of the random component and $\bar{\mathbf{H}}$ is a Rayleigh $N_r \times N_t$ matrix whose entries are complex i.i.d Gaussian random variables with zero mean and unit variance.

2.2. Nakagami-m fading channels

As mentioned in Section 1, various researchers have analyzed the performance of several MIMO schemes under the Nakagami-m fading environment by considering the assumption that phase distribution is uniform. For a Nakagami fading the very special case of uniform distribution is defined when $m = 1$ and it resembles the Rayleigh fading environment. Similarly when $m = \infty$, Nakagami fading diminishes to a nonfading additive white Gaussian noise (AWGN) environment. It tends to resemble Hoyt distribution (also known as Nakagami-q distribution) if the value of m is less than 1 [9].

The behavior of Nakagami-m distribution is mainly used to describe channels perturbed by rapid to mild fading. In this work we investigate the performance of DSM scheme over more realistic non uniform phase distributed Nakagami-m fading channel [9,13] and [16].

The channel matrix for Nakagami-m fading is formulated using [9]

$$h_{r,t} = \sqrt{\sum_{i=1}^{m} \left|\mathbb{Z}_i^R\right|^2} + j\sqrt{\sum_{i=1}^{m} \left|\mathbb{Z}_i^I\right|^2}. \tag{7}$$

$\mathbb{Z}_i^R$, $\mathbb{Z}_i^I$ are circularly symmetric i.i.d Gaussian random variable with zero mean and variance is equal to $\sigma_{\mathbb{Z}}{}^2 = 1/(2m)$ and m is the Nakagami parameter.

The envelope of the Nakagami-m fading channel is distributed as shown below

$$p(\varpi) = \frac{2m^m \varpi^{2m-1}}{\Gamma(m)} e^{(-m\varpi^2)} \tag{8}$$

where $\Gamma(\cdot)$ is the Gamma function and ϖ is a random variable.

Additionally, we define PDF of the phase according to real time investigations as demonstrated in [16]

$$p(\phi) = \frac{\Gamma(m)|\sin(2\phi)|^{m-1}}{2^m \Gamma^2\left(\frac{m}{2}\right)}. \tag{9}$$

where ϕ is the phase corresponding to Nakagami-m distribution. Our major interest is to analyze and quantify the performance of DSM scheme with P-CSI and Imp-CSI. This channel model is in accordance with that shown in [12]. Here we have considered estimate of the channel $\mathbf{H}$ to be $\hat{\mathbf{H}}$ and that $\mathbf{H}$ and $\hat{\mathbf{H}}$ both are jointly ergodic and stationary Gaussian random processes. Moreover, we expect estimate of the channel $\hat{\mathbf{H}}$ and estimation error $\mathbf{E}$ are orthogonal to each other and can be written analytically as

$$\mathbf{H} = \hat{\mathbf{H}} + \mathbf{E}. \tag{10}$$

$\mathbf{E}$ is defined to be complex Gaussian with zero mean and variance $\sigma_e{}^2$. Note that $\sigma_e{}^2$ is the variance parameter that subjugates the condition of channel estimation.

2.3. Optimal ML and suboptimal OB-MMSE decoding strategies for DSM

In this section two decoding strategies have been employed namely optimal ML and suboptimal OB-MMSE detection which is used to reduce the complexity of search space.

2.3.1. Optimal ML detection

Optimal ML detection is used to distinguish the symbols and to achieve the better BER performance for the considered DSM scheme. The antenna indices (A_1, A_2) and information symbols $(\mathbf{s_1}, \mathbf{s_2})$ which were transmitted from the combination of active antennas are detected at the receiver side. Joint estimation of these antenna indices and MQAM information symbols are estimated over an exhaustive ML search metric of $N_t{}^2 M^2$.

$$[\widehat{\mathbf{s}_1}, \widehat{\mathbf{s}_2}, \widehat{A_1}, \widehat{A_2}] = arg \min_{\mathbf{s}_1, \mathbf{s}_2, A_1, A_2,} \left\|\mathbf{Y} - (\mathbf{h}_{\mathbf{A_1}}\mathbf{s_1} + \mathbf{h}_{\mathbf{A_2}}\mathbf{s_2}\mathbf{e}^{\mathbf{j}\theta})\right\|_F^2 \tag{11}$$

$\|\bullet\|_F$ is the Frobenius norm.

2.3.2. Suboptimal OB-MMSE detection

Although ML produces the optimal solution for decoding or detection, nevertheless the complexity of ML system increases exponentially with the increase in number of transmit antennas. This hinders its implementation in practical systems. Yue Xiao et al. proposed a low complexity decoder scheme which has a stable trade-off between complexity and the error performance.

A modified OB-MMSE algorithm for use in DSM systems is presented in this section. Following Yue Xiao et al. the received vector is first to processed to determine the transmit antenna combinations (TACs). Pseudo inverse of each channel has been computed to evaluate z .

Let $\mathbf{y}$ denote the received vector, $\mathbf{H}$ denote the channel matrix, N_t denote the total number of transmit antennas, $\mathbf{N_A}$ denote the number of active antennas. For a DSM scheme the number of active antennas is equal to two. $I = (I_1, I_2, I_3, \ldots, I_N)$ is the set of N_A active transmit antenna combinations in the ith TAC , $V_{th} = 2N_R\sigma^2$ is the threshold value.

In OB-MMSE, TACs are first sorted out based on the reliability of each TAC. After getting the ordered set of TACs, best matched TAC is chosen to find the corresponding transmit symbol. Detailed description and pseudo code is given in [15].

$$z = \begin{bmatrix} z_1, & z_2, & . & . & ., & z_{N_T} \end{bmatrix}^T,$$

$$z_k = (h_k)^{\dagger} y, \quad (h_k)^{\dagger} = \frac{h_k^H}{h_k^H h_k}$$

$$w = [w_1, \quad w_2, \quad . \quad . \quad ., \quad w_N \quad]^T,$$

$$w_i = \sum_{k=1}^{N_P} z_{i_k}^2, \quad i \ \epsilon \ \{1, 2, \ldots, N\}.$$

In order to find the TAC vector, block MMSE equalization procedure has been followed. Specifically, for every conceivable transmit antenna combinations, a simplified block MMSE identifier criterion as shown in [15] is utilized to identify symbols and can be accomplished by using the digital demodulator function. The implementation of OB-MMSE is modified for detection of DSM symbols.

$$\widetilde{\mathbf{s}_{j1}} = Q_1 \left(\left(\left(\mathbf{H}_{I_{k_i}} \right)^{\mathbf{H}} \mathbf{H}_{I_{k_i}} + \sigma^2 I \right)^{-1} \left(\mathbf{H}_{I_{k_i}} \right)^{\mathbf{H}} \mathbf{y}_1 \right)$$

$$\widetilde{\mathbf{s}_{j2}} = Q_2 \left(\left(\left(\mathbf{H}_{I_{k_i}} \right)^{\mathbf{H}} \mathbf{H}_{I_{k_i}} + \sigma^2 I \right)^{-1} \left(\mathbf{H}_{I_{k_i}} \right)^{\mathbf{H}} \mathbf{y}_2 \right)$$

$$\widetilde{\mathbf{s}_j} = \widetilde{\mathbf{s}_{j1}}, \widetilde{\mathbf{s}_{j2}}.$$

Due to the rotation angle introduced in the second transmit symbol in DSM, rotated constellation map has to be considered in its detection. We define digital modulator functions $Q_1(\cdot)$ and $Q_2(\cdot)$ with respect to the MQAM and rotated MQAM constellation maps. Succeeding steps which involve mapping the information symbols to TACs are similar to those used in [15].

$$d_j = \left\| \mathbf{Y} - \mathbf{H}_{I_{k_i}} \widetilde{\mathbf{s}_j} \right\|_F^2.$$

3. Analytical treatment for DSM under fading scenarios

Analytical framework for the ABEP of DSM system under Rayleigh, Rician and Nakagami-m fading environments with P-CSI and Imp-CSI has been derived in this section.

The ABEP can be expressed in terms of Pairwise Error Probability (PEP) between two vectors $\mathbf{S}$ and $\hat{\mathbf{S}}$. When the vector $\mathbf{S}$ is transmitted and it is erroneously detected as $\hat{\mathbf{S}}$, then conditional pairwise error probability (CPEP) can be calculated as shown in [14,18,19] and [20].

3.1. Case 1: Perfect-CSI

$$CPEP(\mathbf{S} \to \hat{\mathbf{S}}|\mathbf{H}) = \mathbf{P_r}(\|\mathbf{Y} - \mathbf{HS}\|_{\mathbf{F}}^{\mathbf{2}} > \left\|\mathbf{Y} - \mathbf{H}\widehat{\mathbf{S}}\right\|_{\mathbf{F}}^{\mathbf{2}} | \mathbf{H})$$
$$= P_r(\|\mathbf{HS}\|^2 - \left\|\mathbf{H}\hat{\mathbf{S}}\right\|^2 - 2\Re\{\mathbf{Y^H}(\mathbf{HS} - \mathbf{H}\hat{\mathbf{S}})\} > 0).$$

For ease of notation $CPEP(\mathbf{S} \to \hat{\mathbf{S}}|\mathbf{H})$ is denoted as $P\left(\mathbf{S} \longrightarrow \widehat{\mathbf{S}}|\mathbf{H}\right)$. Since the noise is Gaussian distributed CPEP can be expressed as given below.

$$P\left(\mathbf{S} \longrightarrow \widehat{\mathbf{S}}|\mathbf{H}\right) = \frac{1}{\pi} \int_0^{\pi/2} exp\left(\frac{\left\|\mathbf{H}\left(S - \widehat{S}\right)\right\|^2}{4N_0 \sin^2\theta} \right) d\theta. \tag{12}$$

In case of perfect CSI, for Rayleigh channel PEP can be expressed as follows:

$$P\left(\mathbf{S} \longrightarrow \widehat{\mathbf{S}}\right) = \frac{1}{\pi} \int_0^{\pi/2} \left(\frac{\sin^2\theta}{\sin^2\theta + \frac{\|\mathbf{s} - \widehat{\mathbf{s}}\|^2}{4N_0}} \right)^{N_r} d\theta. \tag{13}$$

The closed form expression for DSM systems over Rayleigh fading channel can be derived by using [14] and [19] as follows

$$P_{P-CSI}\left(\mathbf{S} \longrightarrow \widehat{\mathbf{S}}\right) = \frac{1}{2}\left[1 - \mu(c) \sum_{k=0}^{N_r - 1} \binom{2k}{k} \left(\frac{1 - \mu^2(c)}{4} \right)^k \right] \tag{14}$$

$$\mu(c) \triangleq \left(\frac{c_{Rayleigh}}{1 + c_{Rayleigh}} \right) \quad c_{Rayleigh} = \frac{\left\|\mathbf{S} - \widehat{\mathbf{S}}\right\|^2}{4N_0}. \tag{15}$$

For a DSM system under Rician fading channel conditions, (12) reduces to

$$P_{P-CSI}\left(\mathbf{S} \longrightarrow \widehat{\mathbf{S}}\right) = \frac{1}{\pi} \int_0^{\frac{\pi}{2}} \left(\left\{ \times exp\left\{ - \frac{\frac{(1+K)\sin^2\theta}{(1+K)\sin^2\theta + a^2\bar{\gamma}/2}}{\frac{Ka^2\bar{\gamma}/2}{(1+K)\sin^2\theta + a^2\bar{\gamma}/2}} \right\} \right\} \right)^{N_r} d\theta \tag{16}$$

where, $a^2 = \left\|\mathbf{S} - \hat{\mathbf{S}}\right\|_F^2$, $\bar{\gamma}$ is the average SNR per bit given by $\mathrm{E}\left[\frac{|h|^2 E_S}{N_0}\right]$.

$$\bar{\gamma} = \frac{E_S}{N_0}\left(\frac{1 - K}{1 + K} \right). \tag{17}$$

For a DSM system evaluated over Nakagami-m fading channels, (12) reduces to

$$P\left(\mathbf{S} \longrightarrow \widehat{\mathbf{S}}\right) = \frac{1}{\pi} \int_0^{\pi/2} \left(\frac{\sin^2\theta}{\sin^2\theta + \frac{\bar{\gamma}\|\mathbf{s} - \widehat{\mathbf{s}}\|^2}{4N_0}} \right)^{N_r} d\theta \tag{18}$$

$$\bar{\gamma} = \frac{E_S}{N_0}\left(1 - \frac{2}{m}\left[\frac{\Gamma\left(\left(\frac{m}{2}\right) + \frac{1}{2}\right)}{\Gamma\left(\frac{m}{2}\right)} \right]^2 - \left[\frac{\Gamma\left(\frac{m}{2}\right) + \frac{1}{2}}{\Gamma\left(\frac{m}{2}\right) \cdot \frac{\sqrt{m}}{2}} e^{j\frac{\pi}{4}} \right]^2 \right). \tag{19}$$

The closed form expression for Nakagami-m fading channels can be derived by using [19] given by,

$$P_{P-CSI}\left(\mathbf{S} \longrightarrow \widehat{\mathbf{S}}\right) = \frac{1}{2}\left[1 - \mu(c) \sum_{k=0}^{N_r - 1} \binom{2k}{k} \left(\frac{1 - \mu^2(c)}{4 \cdot m} \right)^k \right] \tag{20}$$

$$\mu(c) \triangleq \left(\sqrt{\frac{c_{nak}}{1 + c_{nak}}} \right) \quad c_{nak} = \frac{\bar{\gamma}\left\|\mathbf{S} - \widehat{\mathbf{S}}\right\|^2}{4N_0}. \tag{21}$$

3.2. Case 2: Imperfect-CSI (Variable channel state information)

Following Eq. (12) given in [21] the analysis can be extended to DSM systems.

$$P\left(\mathbf{S}\longrightarrow\widehat{\mathbf{S}}\right)=\frac{1}{\pi}\int_{0}^{\pi/2}exp\left(\frac{E_s\left\|\mathbf{H}\left(\mathbf{S}-\widehat{\mathbf{S}}\right)\right\|^2}{4\cdot\left(E_s\cdot\sigma_e^2+\sigma_n^2\right)\sin^2\theta}\right)d\theta. \quad (22)$$

From the above analysis of Case-1 (13) can be re-written as

$$P\left(\mathbf{S}\longrightarrow\widehat{\mathbf{S}}\right)=\frac{1}{\pi}\int_{0}^{\pi/2}\left(\frac{\sin^2\theta}{\sin^2\theta+\frac{\|\mathbf{S}-\widehat{\mathbf{S}}\|^2}{4\cdot\left(E_s\cdot\sigma_e^2+\sigma_n^2\right)}}\right)^{N_r}d\theta. \quad (23)$$

The closed form expression for DSM systems over Rayleigh fading channel with Imp-CSI is given by

$$P_{Imp-CSI}\left(\mathbf{S}\longrightarrow\widehat{\mathbf{S}}\right)=\frac{1}{2}\left[1-\mu\left(c\right)\sum_{k=0}^{N_r-1}\binom{2k}{k}\left(\frac{1-\mu^2\left(c\right)}{4}\right)^k\right] \quad (24)$$

$$\mu\left(c\right)\triangleq\left(\frac{c_{Rayleigh}}{1+c_{Rayleigh}}\right)\quad c_{Rayleigh}=\frac{\left\|\mathbf{S}-\widehat{\mathbf{S}}\right\|^2}{4\cdot\left(E_s\cdot\sigma_e^2+\sigma_n^2\right)} \quad (25)$$

where, $\sigma_e^2=\frac{1}{SNR}$, σ_n^2 is the noise variance.

DSM system under Rician fading channel conditions with Imp-CSI, is given by

$$P_{Imp-CSI}\left(\mathbf{S}\longrightarrow\widehat{\mathbf{S}}\right)=\frac{1}{\pi}\int_{0}^{\frac{\pi}{2}}\left(\left\{\frac{(1+K)\sin^2\theta}{(1+K)\sin^2\theta+a^2\bar{\gamma}/2}\times exp\left\{-\frac{Ka^2\bar{\gamma}/2}{(1+K)\sin^2\theta+a^2\bar{\gamma}/2}\right\}\right\}\right)^{N_r}d\theta \quad (26)$$

where, $a^2=\left\|\mathbf{S}-\hat{\mathbf{S}}\right\|_F^2$, $\bar{\gamma}$ is the average SNR per bit given by $\mathrm{E}\left[\frac{|h|^2E_S}{\left(E_s\cdot\sigma_e^2+\sigma_n^2\right)}\right]$.

$$\bar{\gamma}=\frac{E_S}{\left(E_s\cdot\sigma_e^2+\sigma_n^2\right)}\left(\frac{1-K}{1+K}\right). \quad (27)$$

DSM system over Nakagami-m fading channel conditions with Imp-CSI is given by,

$$P_{Imp-CSI}\left(\mathbf{S}\longrightarrow\widehat{\mathbf{S}}\right)=\frac{1}{2}\left[1-\mu\left(c\right)\sum_{k=0}^{N_r-1}\binom{2k}{k}\left(\frac{1-\mu^2\left(c\right)}{4\cdot m}\right)^k\right] \quad (28)$$

$$\mu\left(c\right)\triangleq\left(\sqrt{\frac{c_{nak}}{1+c_{nak}}}\right)\quad c_{nak}=\frac{\overline{\gamma}\left\|\mathbf{S}-\widehat{\mathbf{S}}\right\|^2}{4\cdot\left(E_s\cdot\sigma_e^2+\sigma_n^2\right)}. \quad (29)$$

4. Simulation results and observations

In this section, two spectral efficiencies were targeted for DSM as well as variants of SM schemes. First set comprises of N_t=4, N_r=4, yielding a spectral efficiency $\eta = 8$ bps/Hz. The second set comprises of N_t=8, N_r=8 and produces a spectral efficiency $\eta = 10$ bps/Hz. For the simulations, a minimum of 10^6 channel realizations have been considered for the ABER estimation. These values are compared with the derived mathematical upper bound. Analytical BER performance of the DSM scheme over Rayleigh, Rician, Nakagami-m fading channels has been substantiated through

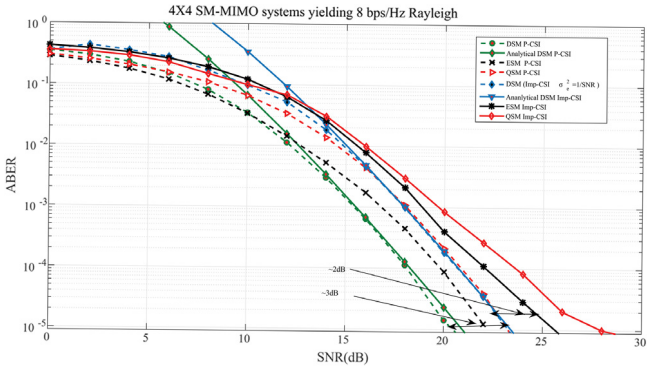

Fig. 2. BER performance analysis of DSM in Imp-CSI ($\sigma_e^2=\frac{1}{SNR}$) and variants of SM schemes (DSM,ESM,QSM) over a Rayleigh fading environment with $N_t=4$, $N_r=4$, yielding η = 8 bps/Hz.

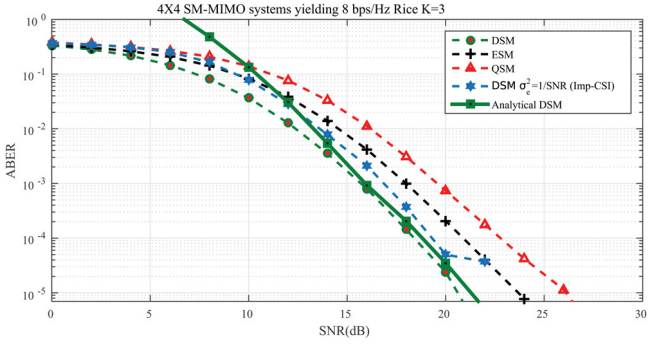

Fig. 3. BER performance analysis of DSM in Imp-CSI ($\sigma_e^2=\frac{1}{SNR}$) and variants of SM schemes (DSM,ESM,QSM) in P-CSI over a Rician fading environment ($K=3$) with $N_t=4$, $N_r=4$, yielding η = 8 bps/Hz.

Monte Carlo simulations. A close correlation is observed between simulation and analytic results. The BER values under conditions of P-CSI and Imp-CSI has been plotted. It is observed that ABER performance of the DSM scheme is superior to other conventional SM schemes.

In Fig. 2, we have shown the BER performance comparison of a DSM scheme with variants of SM (QSM and ESM) for a 4×4 MIMO arrangement yielding a spectral efficiency $\eta = 8$ bps/Hz over a Rayleigh fading channel. It has been observed that DSM system outperforms ESM and QSM systems by 1.8 dB and 2.3 dB respectively in P-CSI environment. If the channel is imperfect ($\sigma_e^2=\frac{1}{SNR}$) there exists a performance deterioration of about 2 dB in comparison to DSM system with P-CSI under lower SNR regime. Amount of performance degradation increases with increase in the value of SNR. Additionally, DSM scheme in Imp-CSI scenario perform better by about 2 dB over ESM systems and 3.5 dB over QSM systems which possesses Imp-CSI. Finally, simulations were terminated for the error floor value of (9×10^{-6}).

Fig. 3, compares the BER performance of DSM scheme with variants of SM (QSM and ESM) for a 4×4 MIMO arrangement yielding a spectral efficiency η = 8 bps/Hz over a Rician fading channel with $K=3$. Close examination of this figure reveals that, DSM system with P-CSI outperforms ESM and QSM systems by 1.9 dB and 2.7 dB respectively. On comparing DSM performance in Imp-CSI condition with P-CSI a degradation of about 1.6 dB is observed in lower SNR regime. Amount of performance degradation increases with higher values of SNR which is similar to that observed in Rayleigh fading. Furthermore, it is noted that the DSM scheme under Imp-CSI scenario performs better by approximately 2 dB and 3 dB over ESM and QSM systems with P-CSI respectively.

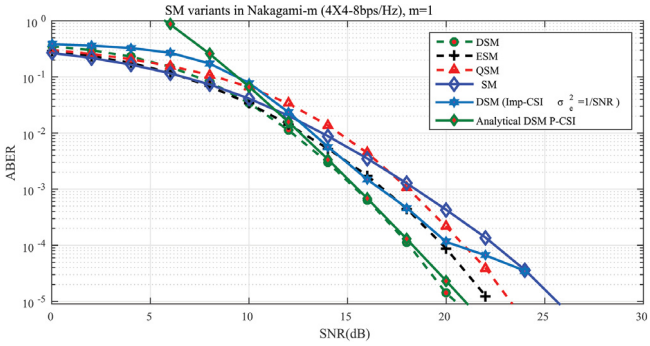

Fig. 4. BER performance analysis of DSM in Imp-CSI ($\sigma_e^2 = \frac{1}{SNR}$) and variants of SM schemes (DSM,ESM,QSM,SM) in P-CSI over Nakagami-m fading environment ($m = 1$) with $N_t = 4$, $N_r = 4$, yielding η = 8 bps/Hz.

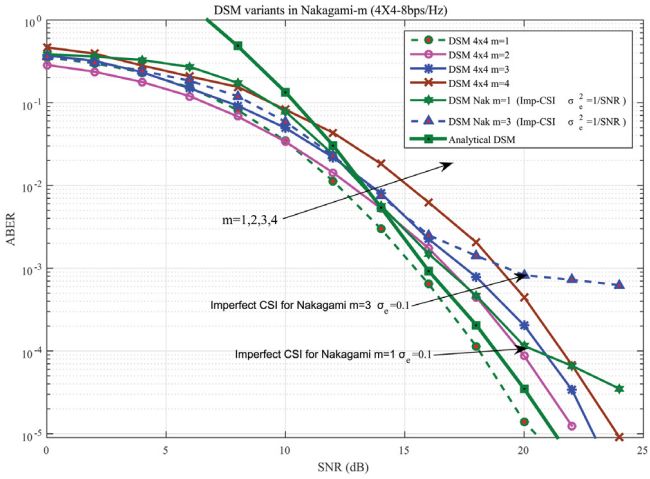

Fig. 5. BER performance analysis of DSM in Imp-CSI ($\sigma_e^2 = \frac{1}{SNR}$) ($m = 1, 3$) and DSM in P-CSI over Nakagami-m fading environment ($m = 1, 2, 3, 4$) with $N_t = 4$, $N_r = 4$, yielding η = 8 bps/Hz.

Finally, simulations were terminated at the error floor value of (6×10^{-5}).

Fig. 4, illustrates the relative performance of SM variants for a 4×4 MIMO arrangement yielding a spectral efficiency of 8 bps/Hz over a Nakagami-m fading channel with $m = 1$. It is observed that DSM outperforms QSM, ESM and SM systems by approximately 1.9 dB, 2.7 dB and 4 dB respectively. It is also seen that DSM scheme under Imp-CSI scenario performs better by approximately 1.3 dB over QSM system and 2.1 dB over SM systems with P-CSI availability. The performance of DSM in Imp-CSI has a downfall of about 1.9 dB when compared to DSM with P-CSI for low SNR values.

A 4×4 MIMO DSM system which produces 8 bps/Hz is compared in Fig. 5. Fig. 5 demonstrates the effect of various channel parameters such as $m = 1, 2, 3, 4$ and the idea of non uniform phase distribution on the performance of DSM scheme over Nakagami fading channel . The instance of $m = 1$ relates to Rayleigh fading and the result is similar to the one revealed in [14] . The performance deterioration of at least 1 dB is observed for every increasing value of m. In order to show the incremental error floor values under Imp-CSI scenario, here we have simulated DSM for $m = 1$ and $m = 3$, Performance degradation of about 3 dB is observed from the value of $m = 1$ to $m = 3$.

Fig. 6 gives the performance analysis of DSM and other variants of SM schemes in Nakagami-m fading environment with $m = 4$. At lower SNR values SM system outperforms all the other variants but in higher SNR values DSM scheme gives the best performance.

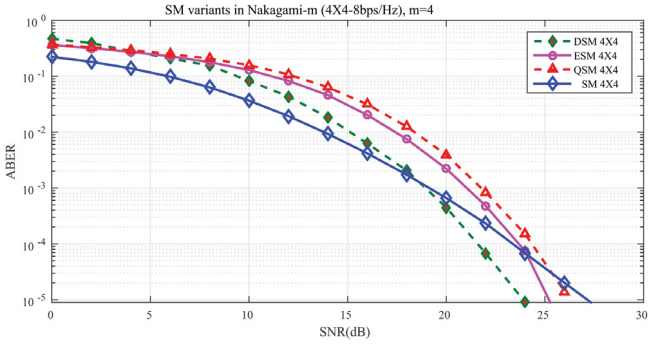

Fig. 6. BER performance analysis of DSM and variants of SM schemes (ESM,QSM and SM) in P-CSI over Nakagami-m possesses non-uniform fading environment ($m = 4$) with $N_t = 4$, $N_r = 4$, yielding η = 8 bps/Hz.

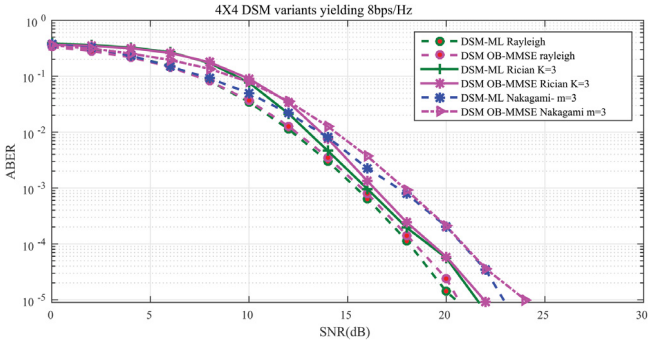

Fig. 7. BER performance analysis of DSM schemes in Rayleigh, Rician and Nakagami-m fading environments comparison of ML and OB-MMSE with $N_t = 4$, $N_r = 4$, yielding η = 8 bps/Hz.

This characteristic of both the frameworks can be justified as follows. At lower SNR values the error in distinguishing the active antenna index dominates, whereas at high SNR values the information symbol error detection predominates. It is also observed that at high values of SNR, DSM system outperform SM scheme by approximately 3 dB.

The comparison of performance of ML and OB-MMSE detection strategies for a DSM system has been demonstrated in Fig. 7. Varied fading channel environments such as Rayleigh, Rician and Nakagami-m are considered for simulation. Close observation of Fig. 7 indicates that for pragmatic values, OB-MMSE performance is almost comparable to ML decoding strategy. At the same time OB-MMSE also provides a 80% reduction in computational complexity over ML detection strategies [15].

In Fig. 8, we have shown the BER performance comparison of a DSM scheme for a 8×8 MIMO arrangement. DSM employs 4 QAM to produce a spectral efficiency η=10 bps/Hz over a Nakagami-m fading channel. The performance deterioration of at least 1 dB is observed for every increasing value of m. The examined results follow the similar trend that was contemplated in Fig. 5. The final set of results reported in Fig. 9 delineate the effect of Nakagami-m channel phase distribution on the execution of DSM frameworks. The realistic non uniform phase parameter with phase $m = 2, 4$ is plotted. When considering uniform phase distribution and expanding value of m, the DSM execution upgrades by an amount of almost 3 dB. The results indicate approximately 4.5 dB improvement for non uniform phase distributed DSM system over uniform phase with $m = 4$. Similarly, when the value of m is reduced the performance gap between the plots increases to approximately 7 dB.

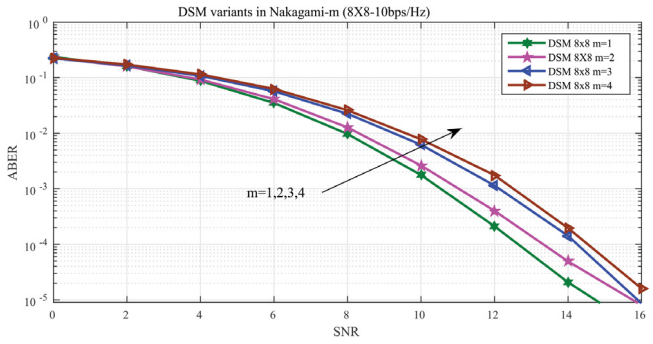

Fig. 8. BER performance analysis of DSM in P-CSI over Nakagami-m fading environment ($m = 1, 2, 3, 4$) with $N_t = 8$, $N_r = 8$, yielding η = 10 bps/Hz.

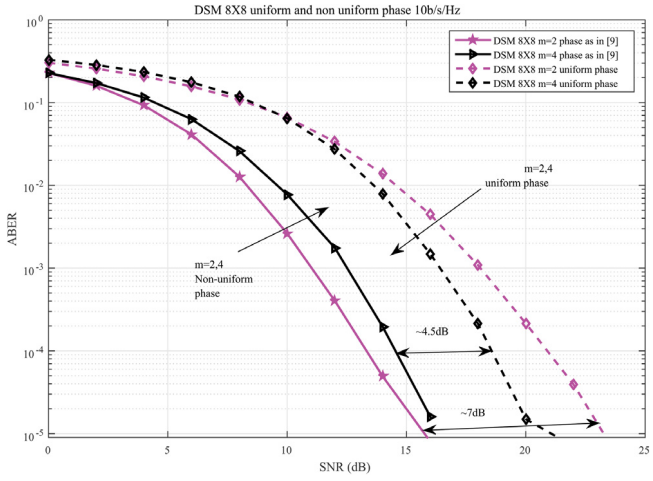

Fig. 9. BER performance analysis of DSM in P-CSI over Nakagami-m fading environment ($m = 2, 4$) comprising uniform and non-uniform phase distribution with $N_t = 8$, $N_r = 8$, yielding η = 10 bps/Hz.

5. Conclusions

DSM is a high rate spectrally efficient MIMO scheme proposed recently. We have designed DSM schemes to work efficiently under conditions of P-CSI and Imp-CSI for channels perturbed by Rayleigh, Rician and Nakagami-m distributions. The ABER performance under these conditions is also evaluated analytically. DSM system shows exceptional performance improvement of the order of 2 dB for different system configurations and channel parameters. Considering that phase distribution associated with the Nakagami distribution is non uniform, the second part of the work deals with evaluating the performance of DSM schemes under channels perturbed by Nakagami-m distribution for varying values of m. Under conditions of non uniform phase distributed Nakagami channels an increase in the value of m results in performance deterioration of the order of approximately 1 dB. In the case of Nakagami channel with uniform phase distribution performance improvement is observed with the increasing values of m. DSM scheme outperforms all the conventional SM schemes by at least 2 dB, over all possible channel environments. This is true irrespective of whether CSI is perfectly or imperfectly available. Finally, modified suboptimal OB-MMSE algorithm is designed for a DSM scheme which gives a near ML performance with reduced computational complexity. Hence these schemes can be advantageously deployed in the next generation 5G wireless communication systems as a realistic and efficient modulation technique.

Acknowledgment

This research work was supported by the project entitled "Uncoordinated Secure and Energy Aware Access in Distributed Wireless Networks" sponsored by Information Technology Research Academy (ITRA) Media Lab Asia, Mumbai vide grant no. ITRA/15(64)/Mobile/USEAADWN/01 dated September 19,2013.

References

[1] V. Tarokh, N. Seshadri, A.R. Calderbank, Space-time codes for high data rate wireless communication: Performance criterion and code construction, IEEE Trans. Inf. Theory 44 (2) (1998) 744–765.
[2] V. Tarokh, H. Jafarkhani, A.R. Calderbank, Space-time block codes from orthogonal designs, IEEE Trans. Inf. Theory 45 (5) (1999) 1456–1467.
[3] S.M. Alamouti, A simple transmit diversity technique for wireless communications, IEEE J. Sel. Areas Commun. 16 (8) (1998) 1451–1458.
[4] E. Basar, Index modulation techniques for 5G wireless networks, IEEE Commun. Mag. 54 (7) (2016) 168–175.
[5] R.Y. Mesleh, H. Haas, S. Sinanovic, C.W. Ahn, S. Yun, Spatial modulation, IEEE Trans. Veh. Technol. 57 (4) (2008) 2228–2241.
[6] M. Di Renzo, H. Haas, A. Ghrayeb, S. Sugiura, L. Hanzo, Spatial modulation for generalized MIMO: Challenges, opportunities, and implementation, Proc. IEEE 102 (1) (2014) 56–103.
[7] A. Stavridis, S. Sinanovic, M. Di Renzo, H. Haas, P. Grant, An energy saving base station employing spatial modulation, in: 2012 IEEE 17th International Workshop on Computer Aided Modeling and Design of Communication Links and Networks (CAMAD), IEEE, 2012, pp. 231–235.
[8] Y. Lee, S. Yun, et al., Interchannel interference avoidance in mimo transmission by exploiting spatial information, in: IEEE 16th International Symposium on Personal, Indoor and Mobile Radio Communications, 2005, Vol. 1, PIMRC 2005, IEEE, 2005, pp. 141–145.
[9] A. Younis, Spatial Modulation: Theory to Practice, The University of Edinburgh, 2014.
[10] R. Mesleh, S.S. Ikki, H.M. Aggoune, Quadrature spatial modulation, IEEE Trans. Veh. Technol. 64 (6) (2015) 2738–2742.
[11] C.-C. Cheng, H. Sari, S. Sezginer, Y.T. Su, Enhanced spatial modulation with multiple signal constellations, IEEE Trans. Commun. 63 (6) (2015) 2237–2248.
[12] R. Mesleh, S.S. Ikki, On the impact of imperfect channel knowledge on the performance of quadrature spatial modulation, in: 2015 IEEE Wireless Communications and Networking Conference (WCNC), IEEE, 2015, pp. 534–538.
[13] A. Younis, R. Mesleh, H. Haas, Quadrature spatial modulation performance over Nakagami-m fading channels, IEEE Trans. Veh. Technol. 65 (12) (2016) 10227–10231.
[14] Z. Yigit, E. Basar, Double spatial modulation: A high-rate index modulation scheme for MIMO systems, in: Wireless Communication Systems (ISWCS), IEEE, 2016, pp. 347–351.
[15] Y. Xiao, Z. Yang, L. Dan, P. Yang, L. Yin, W. Xiang, Low-complexity signal detection for generalized spatial modulation, IEEE Commun. Lett. 18 (3) (2014) 403–406.
[16] M.D. Yacoub, Nakagami-m phase-envelope joint distribution: an improved model, in: 2009 SBMO/IEEE MTT-S International Microwave and Optoelectronics Conference (IMOC), IEEE, 2009, pp. 335–339.
[17] M. Koca, H. Sari, Performance analysis of spatial modulation over correlated fading channels, in: 2012 IEEE Vehicular Technology Conference, VTC Fall, IEEE, 2012, pp. 1–5.
[18] T.M. Duman, A. Ghrayeb, Coding for MIMO Communication Systems, John Wiley & Sons, 2008.
[19] M.K. Simon, M.-S. Alouini, Digital Communication Over Fading Channels, Vol. 95, John Wiley & Sons, 2005.
[20] A. Forenza, D.J. Love, R.W. Heath, A low complexity algorithm to simulate the spatial covariance matrix for clustered mimo channel models, in: 2004 IEEE 59th Vehicular Technology Conference, 2004, Vol. 2, VTC 2004-Spring, IEEE, 2004, pp. 889–893.
[21] O.S. Badarneh, R. Mesleh, S.S. Ikki, H.M. Aggoune, Performance analysis of space modulation techniques over alpha-mu fading channels with imperfect channel estimation, in: 2014 IEEE 80th Vehicular Technology Conference, VTC Fall, IEEE, 2014, pp. 1–5.

Goutham Simha G.D. received his M.Tech. degree in digital electronics and communications in the year 2009 during the same he has worked in LEOs ISRO Bangalore, for a project based on design and implementation of ATP sensor for optical inter-satellite links. Currently he is a Research scholar in the Department of Electronics and Communication Engineering, National Institute of Technology Karnataka, Surathkal, India. He was also part of "Uncoordinated Secure and Energy Aware Access in Distributed Wireless Networks" project which was sponsored by Information Technology Research Academy (ITRA) Media Lab Asia. His areas of interest are: MIMO Wireless communications, Optical Wireless communications and Error Control Coding.

Shriharsha Koila received his B.E. degree in Electronics and Communication Engineering from Malnad College of Engineering (affiliated to VTU), Hassan in 2012 and M.Tech degree from National Institute of Technology Karnataka in 2015. He was part of "Secure Turbulence Resistant Free Space Optical FSO links for Broad Band Wireless Access Networks" project funded by Department of Information Technology India. His research interests are Wireless Communications with emphasis on Error Control Coding applications.

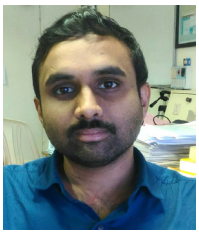

Raghavendra M.A.N.S. received his M.Tech. degree in Communication Engineering from the National Institute of Technology Karnataka, India in 2013. He was involved in "Secure Turbulence Resistant Free Space Optical FSO links for Broad Band Wireless Access Networks" project funded by Department of Information Technology India, and Uncoordinated Secure and Energy Aware Access in Distributed Wireless Networks project which was sponsored by Information Technology Research Academy (ITRA) Media Lab Asia. Currently he is a Research scholar in the Department of Electronics and Communication Engineering, National Institute of Technology Karnataka, India. His areas of interest are: Free Space Optic communications and Error control coding.

U. Shripathi Acharya received his Ph.D. degree from Indian Institute of Science, Bangalore in 2005. He was principal coordinator for "Design and Commissioning of Simulators for the Indian Railway Signaling System (for both Single Line and Double Line Operation)" project (2007–2009), "Secure Turbulence Resistant Free Space Optical FSO links for Broad Band Wireless Access Networks" (2009–2012), " Uncoordinated, Secure and Energy Aware Access in Distributed Wireless Networks" project which was sponsored by Information Technology Research Academy (ITRA) Media Lab Asia (2013–2016) and chief coordinator for project "FIST" (2016–2021). Dr. U. Shripathi Acharya is with National Institute of Technology Karnataka, Surathkal from last 27 years and is currently serving as Professor and Head, Department of Electronics and Communication Engineering. His areas of interest are: Theory and Applications of Error Control Codes, Wireless Communications, Design of Free Space and Underwater Optical Communication Systems.